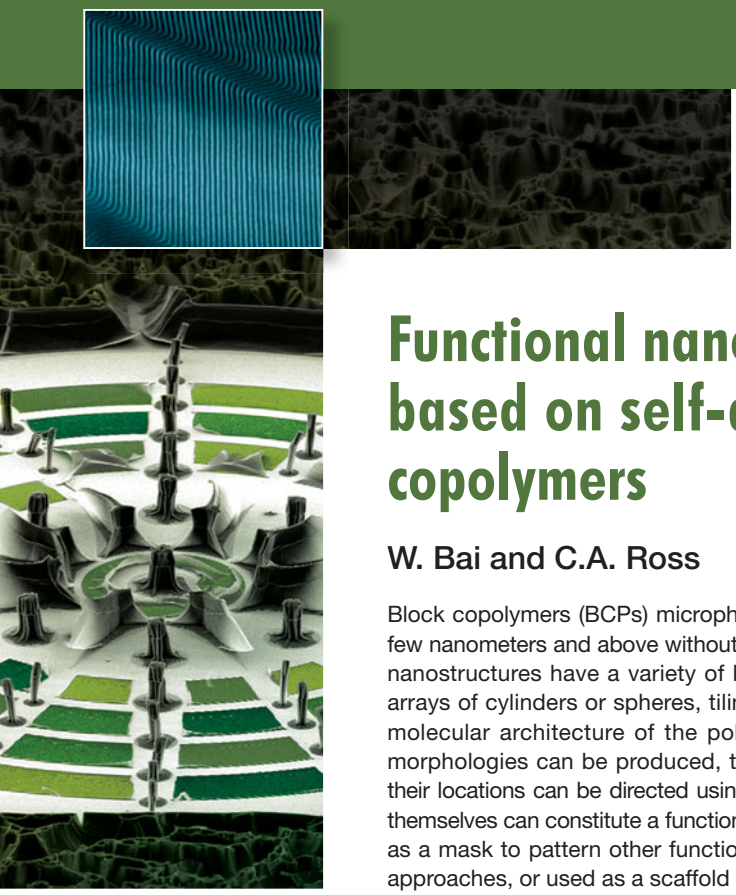


Functional nanostructured materials based on self-assembly of block copolymers

W. Bai and C.A. Ross

Block copolymers (BCPs) microphase-separate to form periodic patterns with periods of a few nanometers and above without the need for lithographic guidance. These self-assembled nanostructures have a variety of bulk geometries, including alternating lamellae, gyroids, arrays of cylinders or spheres, tiling patterns and core–shell structures, depending on the molecular architecture of the polymer and the volume fraction of its blocks. Non-bulk morphologies can be produced, the ordering of the microdomains can be improved, and their locations can be directed using various templates and processing strategies. The blocks themselves can constitute a functional material, such as a photonic crystal, or they can be used as a mask to pattern other functional materials, functionalized directly by various chemical approaches, or used as a scaffold to assemble nanoparticles or other nanostructures. BCPs offer tremendous flexibility in creating nanostructured materials with a range of applications in microelectronics, photovoltaics, filtration membranes, and other devices.

Introduction

A block copolymer (BCP) is a polymer that is made up of blocks of chemically distinct monomers. For example, a polystyrene-*block*-polymethylmethacrylate (PS-*b*-PMMA) BCP consists of a PS chain covalently bonded to a PMMA chain. If the blocks are immiscible, the BCP can self-assemble into periodic nanostructures with dimensions ranging from a few nanometers to several 100 nanometers.[1–5] The phase-separated structure consists of "microdomains" of each block whose geometry depends on the volume fraction of the block and whose periodicity depends on the length of the polymer chain.[6] The periodicity of the structure can range from a few nanometers to hundreds of nanometers.

A rich variety of nanostructures can be self-assembled based on the intrinsic properties of the blocks and the microdomain geometry, which is influenced by the polymer architecture, the annealing process (e.g., annealing by exposure to a solvent vapor environment or to an elevated temperature), and constraints such as those imposed by a patterned substrate.[3,7] BCPs with two chemically distinct blocks (e.g., diblock copolymers [**Figure 1**a–c]) or three (e.g., triblock copolymers) or three (e.g., triblock terpolymers) chemically distinct blocks are most commonly used, but incorporating further blocks and various architectures such as linear, star, cyclic, or brush copolymers brings more diversity to both the properties and the morphology of the resulting self-assembled structure (Figure 1d).[8]

BCPs can be used in a wide range of applications,[9,10] constituting functional materials themselves by virtue of the properties of the blocks, or by selectively etching[11] one block to form masks or templates for the synthesis of functional materials. BCPs can include organic coil-like blocks, liquid-crystalline blocks, Si- or metal-containing blocks, biological blocks, or conductive blocks, thereby providing a multitude of properties.[12–15] The BCP nanostructure can be altered by several chemical methods such as sequential infiltration synthesis (SIS), which introduces metals or oxides from a precursor as in chemical vapor deposition,[16] by salt complexation,[17] or by nanoparticle incorporation.[18]

Many of these applications are based on thin films of BCPs, and one of the most widely studied applications is in nanoscale lithography, where one block is removed by etching, and the other is used as a mask to define features in a microelectronic device (Figure 1a). In this article, we will first discuss the applications of thin-film BCPs in lithography and other fields where a two-dimensional (2D) nanopatterned structure is required. We will then discuss three-dimensional (3D) BCP assemblies. We show that BCP nanostructures have applications in fabrication of integrated circuits,[19,20] magnetic storage media,[21–23] sensors,[24,25] photonic crystals,[26] photovoltaics,[27] and separation membranes,[28] as well as for making 3D nanostructures.[4]

W. Bai, Department of Materials Science and Engineering, Massachusetts Institute of Technology, USA; wbai@mit.edu
C.A. Ross, Department of Materials Science and Engineering, Massachusetts Institute of Technology, USA; caross@mit.edu
DOI: 10.1557/mrs.2016.1

© 2016 Materials Research Society
https://doi.org/10.1557/mrs.2016.1 Published online by Cambridge University Press

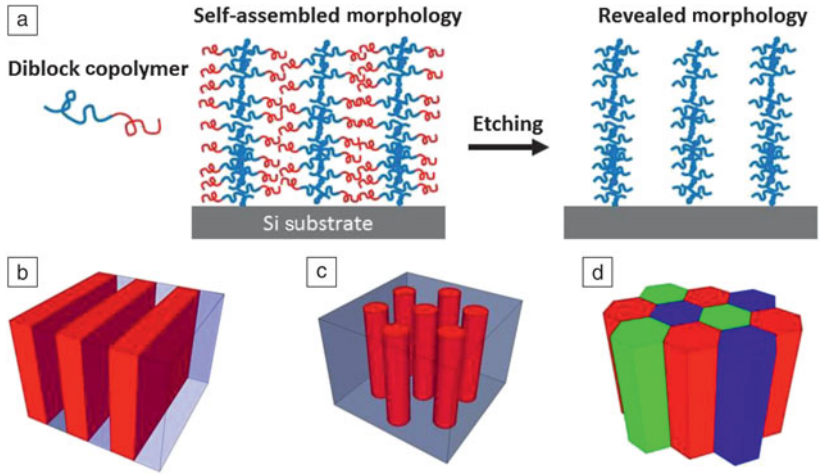


Figure 1. Schematics of block copolymer (BCP) self-assembly. (a) Self-assembled morphology of a diblock copolymer and the morphology revealed after etching one block. (b–d) Representative structures from BCP self-assembly. (b) Lamellae; (c) cylinders, both from a diblock copolymer; (d) Archimedean tiling from a star terpolymer.

BCPs for nanolithography

In nanolithography, a film of a BCP is prepared on a substrate, and one of the blocks is removed. The remaining structure serves as a mask for pattern transfer into a metal, dielectric, or other material. This can be carried out using the microdomain pattern made from an untemplated BCP film, producing a dense array of dots, holes, or lines without long-range order. However, the greatest efforts have been expended in developing BCP nanolithography for nanoscale electronic devices, where precise registration and reproducibility of the self-assembled nanostructures and low defect levels are essential. Conventional 193-nm wavelength photolithography feature sizes are limited by diffraction, although sublithographic feature sizes may be obtained by complex double or quadruple patterning processes.[29] However, 193-nm lithography does not produce features below about 20-nm dimensions, and directed self-assembly (DSA) of BCPs has become a candidate planar process for semiconductor device nanofabrication, according to the International Technology Roadmap for Semiconductors.

The period of the microphase-separated BCP structure is governed by the polymer chain length and hence the degree of polymerization, N (the number of monomers constituting the chain), but the driving force for self-assembly is governed by the product χN, where χ is the Flory–Huggins interaction parameter quantifying the incompatibility between the blocks. Therefore, high χ is desirable to obtain features with small period from BCPs with low N. BCPs that yield a feature period below 10 nm can microphase-separate at room temperature if χ is high enough[30] or by design of the macromolecular architecture (such as brush BCPs). This makes BCP lithography an attractive path to continued device miniaturization.

BCP thin films can be spin-coated from solution like a resist layer, annealed using a hotplate at moderate temperatures or by placing them in a solvent vapor, and etched by reactive ion etching (RIE), making them compatible with conventional semiconductor fabrication technology.[31,32] Diblock copolymer films on unpatterned substrates form periodic morphologies after annealing, consisting of close-packed spheres, in-plane or out-of-plane-oriented cylinders or lamellae, perforated lamellae, or gyroids, by controlling the block volume fraction[1] and the annealing process (**Figure 2**a–c).[7,33]

More diverse morphologies can be produced from tri-BCPs (or multi-BCPs),[8,34] mixtures of di-BCPs,[35] or multi-BCPs blended with a homopolymer.[11] For example, square arrays were achieved by using triblock terpolymer/homopolymer blends (Figure 2d),[11] Archimedean tiling patterns were produced from a three-miktoarm star terpolymer (a star-shaped polymer where three different polymer arms emanate from a core) (Figure 2e),[34] and blended morphologies between spheres and perforated lamellae were

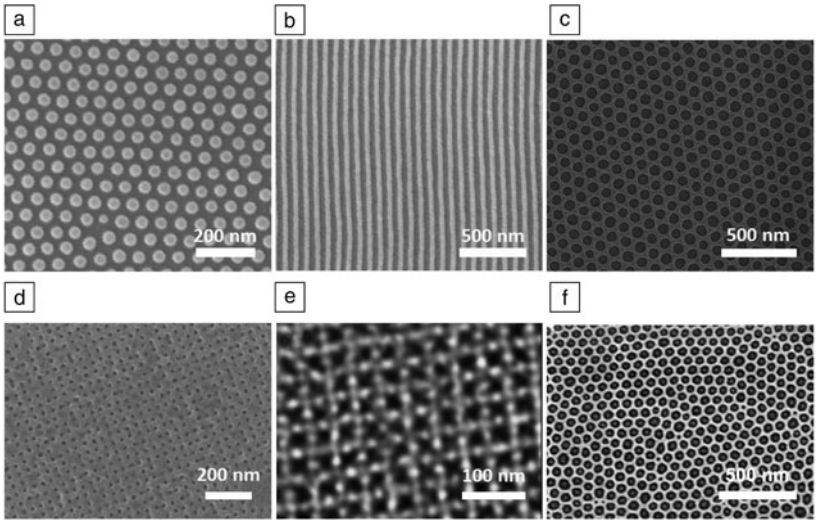


Figure 2. Representative scanning electron microscope images of thin-film self-assembled block copolymer (BCP) structures. (a) Monolayer of spheres; (b) in-plane cylinders; (c) perforated lamellae; (a–c) are from a diblock copolymer. (a–c) Reproduced with permission from Reference 33. © 2014 ACS Publications. (d) Square array of holes from a linear triblock terpolymer blended with a homopolymer. Reproduced with permission from Reference 11. © 2012 ACS Publications. (e) Archimedeam tiling pattern, from a three-miktoarm star terpolymer blended with a homopolymer. Reproduced with permission from Reference 34. © 2013 ACS Publications. (f) Hierarchical nanostructure from a blend of a silicon-containing BCP and an iron-containing BCP. Reproduced with permission from Reference 35. © 2013 Nature Publishing Group.

https://doi.org/10.1557/mrs.2016.1 Published online by Cambridge University Press

demonstrated by blending a Si-containing BCP with an iron-containing BCP (Figure 2f).[35]

The microdomain patterns formed in thin films of BCPs possess short-range order, but lack long-range order, as seen in some of the images in Figure 2. A top-down method can be employed to guide BCP self-assembly, providing registration and alignment with features in the substrate, and minimizing the defectivity. Graphoepitaxy and chemoepitaxy are the two main templating strategies for DSA,[36–40] using physical confinement to direct the arrangement of the polymer chains and interfacial interactions to induce preferential wetting by the polymer chains, respectively, to control BCP self-assembly. This can produce well-ordered periodic arrays as well as aperiodic structures not found in bulk.[41–43] Topographical templates for graphoepitaxy include small posts fabricated by electron-beam lithography, functionalized to be attractive to one block,[44] or trenches fabricated by photolithography or interference lithography.[45–48] On the other hand, chemoepitaxy templates consist of chemically distinct regions of the substrate that are attractive to one or the other block, such as stripes, bends, dots, and other features.[49–51] In both graphoepitaxy and chemoepitaxy, pattern multiplication has been demonstrated (i.e., the density of templating features can be less than the final density of the BCP pattern).[37,49] To optimize the templates in order to produce the desired self-assembled BCP geometries, inverse design algorithms combined with self-consistent field theory (SCFT) simulations have been developed, where SCFT can predict the BCP morphologies for different conditions of film thickness, topographic or chemical confinements, and surface energy.[19,52–54]

Figure 3 shows examples of BCP films templated by graphoepitaxy (Figure 3a–e, g–h) and chemoepitaxy (Figure 3f).[55,56] The scale-up of these processes to the wafer level, using templates made by photolithography, has been demonstrated.[57,58]

As mentioned previously, a high χ is desirable to obtain microdomains with small dimensions. However, high-χ BCPs usually exhibit large differences in surface energy between the blocks, favoring in-plane orientation of lamellar or cylindrical microdomains. Perpendicularly oriented microdomains provide high-aspect-ratio features that facilitate pattern transfer, and can be promoted by a neutral coating that has equal affinity to both blocks of the polymer chain,[59,60] a comb-like polymer architecture,[61] and processing under external conditions, including an electric field,[62] magnetic field,[63] temperature gradient,[64,65] solvent gradient,[60,66] shear,[67] zone casting,[68] electrohydrodynamic jet printing,[69] or electrospray deposition.[70] **Figure 4** shows examples of the alignment of BCP microdomains perpendicular to the substrate.[71]

Pattern transfer from two-dimensional BCP films

In some applications, the BCP film itself forms the functional material, such as a porous dielectric formed by etching a BCP film, but in many cases, the BCP film is used as a sacrificial mask for patterning another material.[72,73] Monolayers of in-plane cylinders or spheres, perpendicular cylinders and lamellae, and perforated lamellae are particularly suitable for pattern transfer. Pattern transfer takes advantage of the

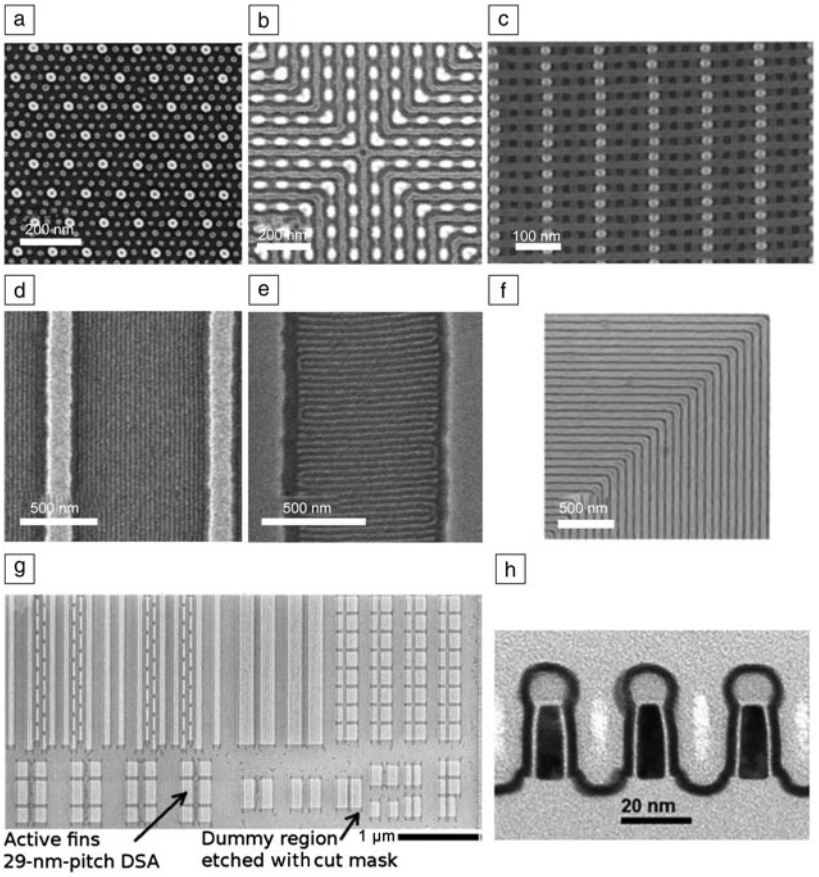


Figure 3. Directed self-assembly (DSA) of block copolymers (BCPs). (a–c) Scanning electron microscope (SEM) images of ordered BCP morphology formed within a sparse 2D lattice of posts (brighter dots). (a) Sphere array. Reproduced with permission from Reference 37. © 2008 AAAS. (b) Nested-elbow structures with a cross-point junction in the center. Reproduced with permission from Reference 55. © 2010 Nature Publishing Group. (c) 3D bilayer cylindrical structure. Reproduced with permission from Reference 44. © 2012 AAAS. SEM images of cylinders (d) parallel and (e) perpendicular to steps on a trenched substrate. (d–e) Reproduced with permission from Reference 56. © 2007 ACS Publications. (f) Top-down SEM of 90°-angled lamellae from chemoepitaxy of a ternary polystyrene-*block*-poly(methyl methacrylate)/polystyrene/polymethyl methacrylate blend. Reproduced with permission from Reference 50. © 2005 AAAS. (g) DSA of a lamellar phase BCP to form line-space circuit patterns in order to fabricate Si fin features. (h) Transmission electron microscope image of 29-nm pitch silicon-on-insulator fins formed by BCP DSA. (g–h) Reproduced with permission from Reference 46. © 2014 ACS Publications.

https://doi.org/10.1557/mrs.2016.1 Published online by Cambridge University Press

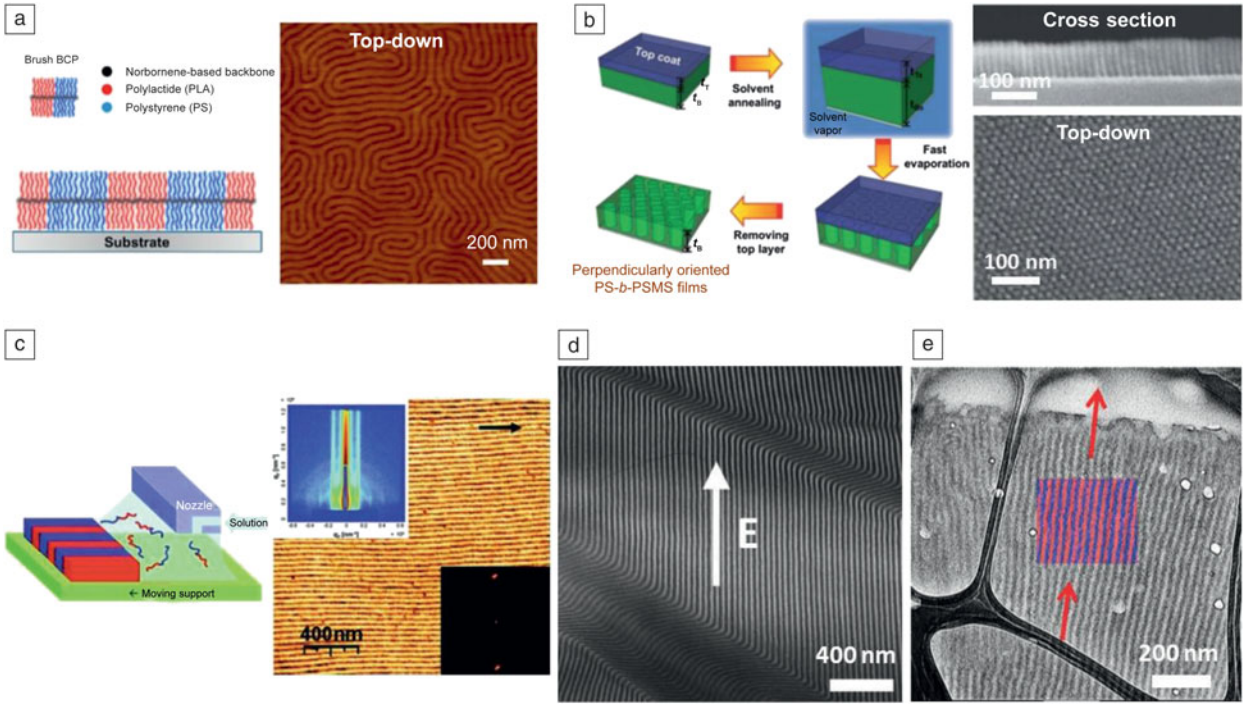


Figure 4. Controlling the orientation of microdomains. (a) Perpendicular microdomains from the self-assembly of a brush block copolymer (BCP). Left: schematic. Right: atomic force microscope image. Reproduced with permission from Reference 61. © 2013 ACS Publications. (b) The solvent annealing of BCP thin films with a top coat layer to produce perpendicular microdomains. Left: schematic, t_A: top coating thickness, t_B: BCP film thickness. Right: Scanning electron microscope image of cross-section and top-down view. Reproduced with permission from Reference 60. © 2014 Wiley-VCH. (c) Zone casting method to direct the self-assembly of BCPs; Left: schematic. Right: atomic force microscope images and grazing incidence small-angle x-ray scattering (upper left inset) patterns of aligned microdomains. Arrow indicates casting direction. Reproduced with permission from Reference 68. © 2011 ACS Publications. (d) Electric-field-induced alignment of BCP microdomains. Reproduced with permission from Reference 71. © 2002 APS. (e) The electrospray process of a tri-BCP. Arrows indicate solvent evaporation direction. Reproduced with permission from Reference 70. © 2015 Wiley-VCH.

methods developed for planar processing, including additive (e.g., liftoff) and subtractive (etching) methods.

Etching an underlying material through a BCP mask allows pattern transfer into many materials, including multilayers or epitaxial structures that cannot be grown on top of the BCP mask.[2,73,74] RIE or ion-beam etching are typically used, and the BCP pattern may first be transferred into a hard mask such as a heavy metal (Ta, W, etc.) or hard carbon, which has greater durability than the BCP film during the etch of the functional material.

Additive patterning has also been widely applied, including electrodeposition, liftoff, and damascene processes.[21,75] Liftoff involves depositing the functional material onto a soluble BCP pattern with vertical or undercut pores, using a collimated vapor deposition process such as evaporation to produce well-defined edge morphologies of the deposited material. Dissolving the BCP pattern removes the material on top of it, leaving only the material that was deposited on the substrate at the bottom of the pores. In a damascene process, the functional material is deposited over BCP topographical features, then etched back and planarized by, for example, RIE. Etching is stopped once it has reached the BCP features, leaving the functional material within the pores of the BCP film.[76]

BCP-based routes to three-dimensional nanostructured materials

BCPs can also produce 3D structures, which can be built up from 2D layers, or formed in one step from thick-film or bulk BCPs with multiple layers of microdomains (**Figure 5**). One class of synthetic routes involves building a 3D functional material from stacks of 2D layers or by repeatedly templating one BCP on another (Figure 5a–c).[4,77] Independent BCP layers can be stacked by separating them, for example, using a graphene or silicon layer in between the layers (Figure 5d).[78,79] The orientation of microdomains in different layers can be controlled independently by shear alignment induced by a laser pulse (Figure 5e),[80] solvent incorporation, a thermal gradient, or direct mechanical shear. This has been used to make lattice structures with arbitrary symmetries from a cylinder-forming BCP.[81,82] Sequential self-assembly processes use the etched, self-assembled BCP microdomains of a lower layer as a new template for an upper layer of the same or different BCP, which can result in a wide range of novel 3D nanostructures.[83] The orientation of one layer of cylinders on another one can be controlled by substrate chemistry and topography.[84] Meshed structures consisting of two layers of cylinders at an angle to each other can also be made in one step by suitable templating (Figure 3c).[44]

https://doi.org/10.1557/mrs.2016.1 Published online by Cambridge University Press

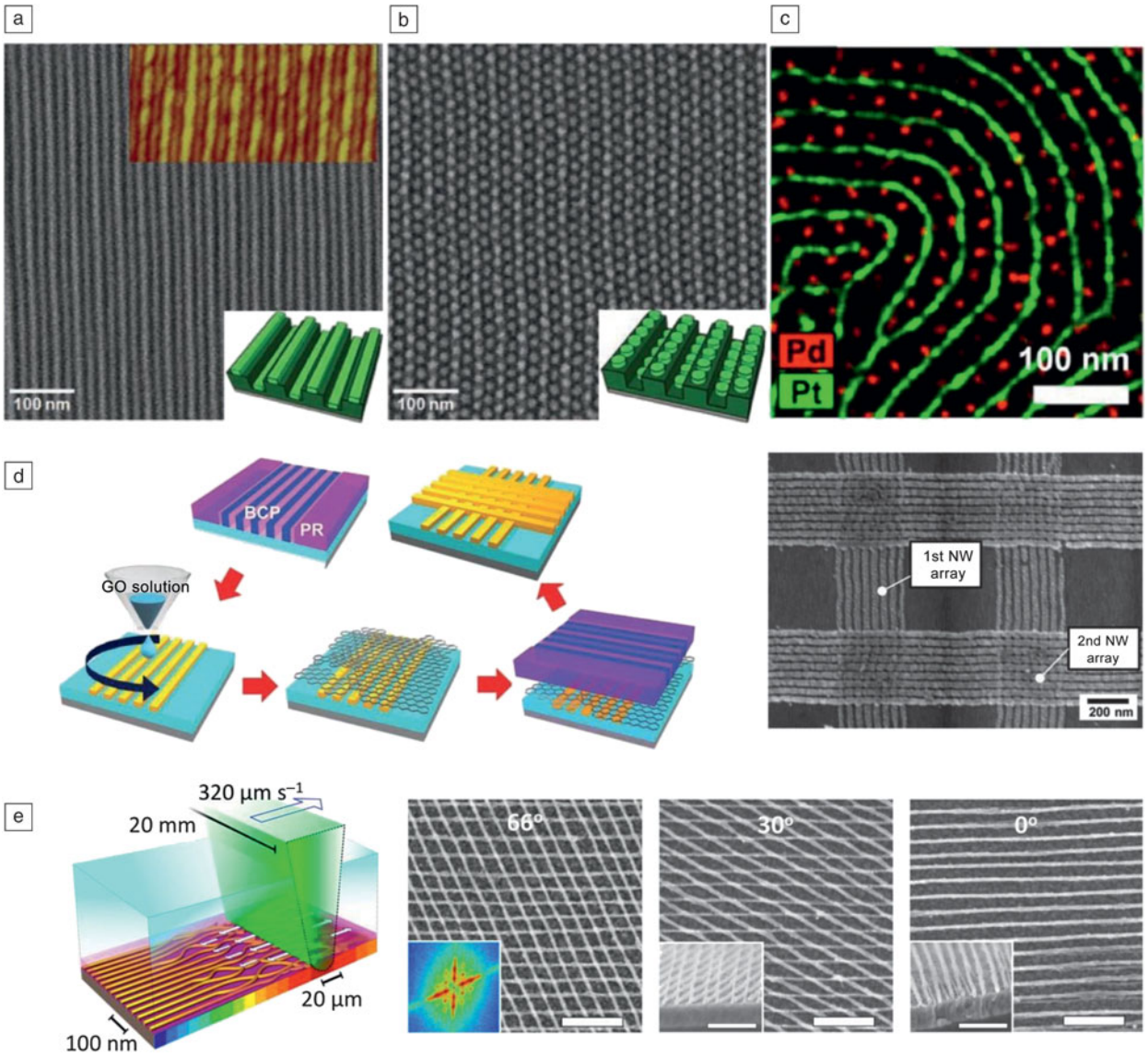


Figure 5. Sequential self-assembly processes. (a–b) Hierarchical line-on-line structures (a) and dots-on-line structures (b) made from a 16-kg mol^{-1} polystyrene-*block*-polydimethylsiloxane (PS-*b*-PDMS) on a 45-kg mol^{-1} PS-*b*-PDMS pattern. Reproduced with permission from Reference 83. © 2011 Wiley-VCH. (c) Multicomponent nanopatterning and elemental mapping of a Pt nanowire-Pd nanodot array made using sequential block copolymer (BCP) self-assembly. Reproduced with permission from Reference 77. © 2013 ACS Publications. (d) Left: schematic of independent control of a double layer of BCP microdomains by inserting a graphene layer in between the BCP layers (PR, photoresist). Right: Al nanowire (NW) crossbar array made from double layers of orthogonally directed self-assembly. Reproduced with permission from Reference 78. © 2013 Wiley-VCH. (e) Soft-shear laser zone annealing, where laser absorption induced both a sharp local temperature raise and mechanical shear from the thermal expansion of the top layer of polydimethylsiloxane. Scale bars 200 nm. Reproduced with permission from Reference 82. © 2015 Nature Publishing Group.

Converting these 3D morphologies into functional materials can be done by a variety of methods. One block can be replaced by another material, for example, by etching it and backfilling by electrodeposition,[85] or by selectively depositing material by SIS[16,86] or chemical reduction.[17] Nanoparticles such as Au can be formed within poly-4-vinylpyridine blocks by reduction of salts.[87] Alternatively, nanoparticles can be synthesized separately and blended with the BCP during casting to produce a co-assembled structure.[88,89]

Functional materials made from BCPs

Nanostructured films made by pattern transfer from a BCP layer using planar processing exhibit a wide range of interesting and useful properties.[90] Some examples of these structures are given in **Figure 6**, including patterned magnetic media (Figure 6a),[23,91] nanowire transistors,[92,93] capacitors,[94] phase-change memories (Figure 6f),[95] resistive memories,[96] or triboelectric generators[97] made using BCPs. Well-ordered BCP microdomain arrays can produce photonic bandgaps spanning

https://doi.org/10.1557/mrs.2016.1 Published online by Cambridge University Press

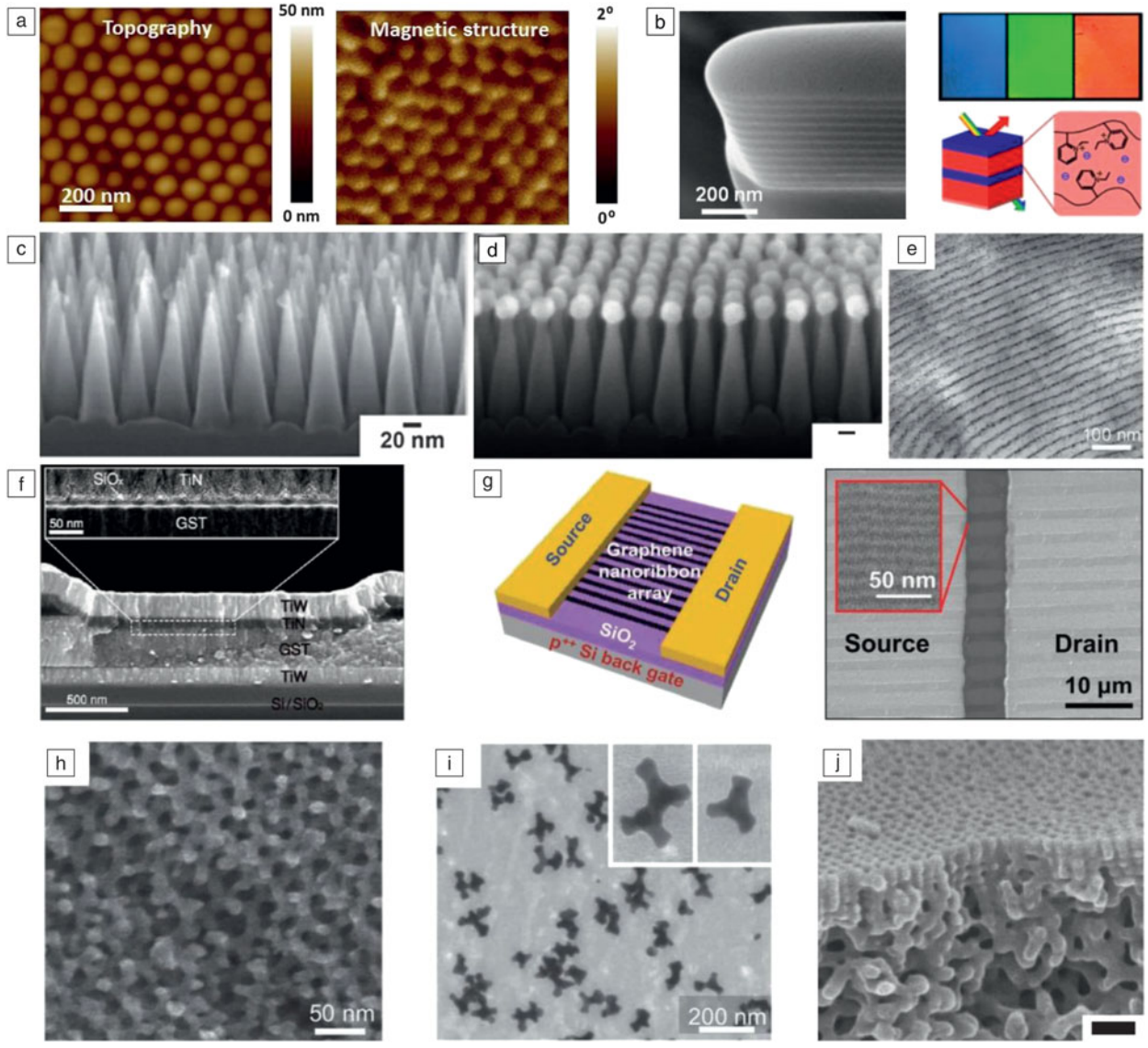


Figure 6. Functional materials made using block copolymers (BCPs). (a) Left: the surface topography of cobalt nanodots. Right: the corresponding magnetic structure showing in-plane magnetization. Reproduced with permission from Reference 73. © 2015 IOPscience. (b) Left: cross-sectional scanning electron microscope (SEM) image of a lamellar BCP film. Right: schematic representation of the mechanism for color change in a photonic lamellar BCP gel, where photonic bandgap was tuned by changing lamellar periodicity in order to control structural coloration. Reproduced with permission from Reference 98. © 2012 ACS Publications. (c–d) Side-view SEM images of a silicon superhydrophobic surface textured with nanocones (c), silicon nanotextured surface (d). (c–d) Scale bars 20 nm. Reproduced with permission from Reference 107. © 2014 Wiley-VCH. (d) Reproduced with permission from Reference 108. © 2015 Nature Publishing Group. (e) Transmission electron microscope image of BCP and nanoparticle co-assembly. Reprinted with permission from Reference 80. © 2012 ACS Publications. (f) Cross-sectional SEM images of a phase-change memory device using a cylindrical BCP nanostructure. GST: $Ge_2Sb_2Te_5$. Reproduced with permission from Reference 95. © 2013 ACS Publications. (g) Schematic of a field-effect transistor based on graphene nanoribbon arrays patterned by BCP lithography and the corresponding SEM image. Reproduced with permission from Reference 93. © 2013 Wiley-VCH. (h) Chiral plasmonic structure made from Au templated in a gyroid triblock terpolymer. Reproduced with permission from Reference 85. © 2011 Wiley-VCH. (i) Branched Au plasmonic structures from seeded electrodeposition in a gyroid BCP. Reproduced with permission from Reference 114. © 2013, Wiley-VCH. (j) Filtration membrane: A sponge-like nanostructure with a vertical channel on top was fabricated from BCP self-assembly. Scale bar is 100 nm. Reproduced with permission from Reference 101. © 2011 ACS Publications.

the entire visible spectrum and with large tunability by swelling (Figure 6b).[98]

In contrast to the precise and intricate structures formed by DSA, some applications only require short-range-ordered nanostructures with or without a common orientation. This is straightforward to accomplish by BCP thin-film self-assembly. Examples include porous dielectrics,[99] such as the IBM Airgap,[100] filtration membranes,[101] or water desalination

https://doi.org/10.1557/mrs.2016.1 Published online by Cambridge University Press

membranes (Figure 6j),[102,103] photovoltaic membranes,[104] and electrodes for batteries.[105,106] Superhydrophobic surfaces have self-cleaning, antireflection, and antibacterial functions and can be produced from nanostructured films of BCPs, such as nanocone textures (Figure 6c),[107] or moth-eye nanostructures (Figure 6d).[108] Amphililic BCPs have been used as building blocks for the preparation of micellar drug carriers.[109]

Nanoparticle inclusion within BCPs can produce a well-ordered morphology in which the orientation and spatial arrangement of the nanoparticles, and thus, their anisotropic physical properties, can be controlled (Figure 6e).[110–112] For example, localized surface plasmon resonance and surface-enhanced Raman scattering from nanorods with ordered arrangement and common orientation can be used for photonics or sensing (Figure 6i).[113,114] A self-assembled BCP nanostructure can be treated as a 3D template after one block is removed, and back-filling of nanoparticles such as those made of transition-metal oxide particles can provide unique electronic, optical, and catalytic properties, useful in applications such as solar cells and batteries (Figure 6h).[85,106]

In a photovoltaic, the donor–acceptor interfaces are critical for photogeneration of charges and device performance.[104,115] Organic solar cells intermix the donor and acceptor material in a bulk heterojunction active layer. A conjugated donor–acceptor BCP can produce a stable active layer morphology based on the block volume fraction and annealing process.[116]

Summary and outlook

We have shown that BCPs offer extensive opportunities for the fabrication of functional materials. This can take advantage of the bulk periodic morphology of the BCP, or of thin films or confined regions of the BCP in which non-bulk morphologies can form. Microdomains can be aligned by applying fields, shear, solvent evaporation, temperature gradients, or substrate topography, and their positions can be precisely controlled by nanoscale graphoepitaxial or chemoepitaxial substrate features. BCPs may themselves be functional, or they can be used as templates to produce other functional materials. Numerous methods exist for pattern transfer, including selective incorporation of nanoparticles, deposition using infiltration or chemical reduction, etching of one block and backfilling, or using a film of the BCP as a mask for planar processes such as etching or liftoff. BCPs enable hierarchical synthesis where one material is templated by another to give a material with different length scales.

There are several important unsolved issues surrounding the use of self-assembled BCPs in the fabrication of functional nanostructures. These include: (1) a lack of theoretical understanding of the BCP self-assembly mechanisms that are associated with specific processing routes, such as solvent vapor annealing, incorporation of nanoparticles, or shear annealing that introduces residual strain, influencing subsequent self-assembly; (2) the ability to precisely control self-assembly to make 3D structures; (3) defects in the self-assembled morphology, in particular, eliminating metastable defects; (4) novel molecular architectures or compositions are needed to realize greater control over the self-assembled morphology and functionality.

BCP-inspired functional materials are already in use or under development for a vast range of applications, including membranes, photovoltaics, and next-generation lithography. Their role will certainly increase as BCP synthesis, processing, and pattern transfer methods improve.

Acknowledgments

The authors gratefully acknowledge financial assistance from C-SPIN, a STARnet Center of SRC supported by DARPA and MARCO, and TSMC.

References

1. F.S. Bates, G.H. Fredrickson, *Annu. Rev. Phys. Chem.* **41**, 525 (1990).
2. R.A. Segalman, *Mater. Sci. Eng. R* **48**, 191 (2005).
3. J.Y. Cheng, C.A. Ross, H.I. Smith, E.L. Thomas, *Adv. Mater.* **18**, 2505 (2006).
4. C.A. Ross, K.K. Berggren, J.Y. Cheng, Y.S. Jung, J.-B. Chang, *Adv. Mater.* **26**, 4386 (2014).
5. A. Nunns, J. Gwyther, I. Manners, *Polymer (Guildf)* **54**, 1269 (2013).
6. M. Hillmyer, *Curr. Opin. Solid State Mater. Sci.* **4**, 559 (1999).
7. C. Sinturel, M. Vayer, M. Morris, M.A. Hillmyer, *Macromolecules* **46**, 5399 (2013).
8. F.S. Bates, M.A. Hillmyer, T.P. Lodge, C.M. Bates, K.T. Delaney, G.H. Fredrickson, *Science* **336**, 434 (2012).
9. F.H. Schacher, P.A. Rupar, I. Manners, *Angew. Chem. Int. Ed. Engl.* **51**, 7898 (2012).
10. H.G. Yoo, M. Byun, C.K. Jeong, K.J. Lee, *Adv. Mater.* **27**, 3982 (2015).
11. H.K. Choi, J. Gwyther, I. Manners, C.A. Ross, *ACS Nano* **6**, 8342 (2012).
12. K. Kulbaba, I. Manners, *Macromol. Rapid Commun.* **22**, 711 (2001).
13. Y. Zhou, S. Ahn, P. Deshmukh, R.M. Kasi, *Liquid Crystalline Block Copolymers; Encyclopedia of Polymer Science and Technology* (Wiley, Hoboken, NJ, 2013).
14. B. Olsen, R. Segalman, *Mater. Sci. Eng. R* **62**, 37 (2008).
15. C.A. Ross, Y.S. Jung, V.P. Chuang, F. Ilievski, J.K.W. Yang, I. Bita, E.L. Thomas, H.I. Smith, K.K. Berggren, G.J. Vancso, J.Y. Cheng, *J. Vac. Sci. Technol. B* **26**, 2489 (2008).
16. Q. Peng, Y.-C. Tseng, S.B. Darling, J.W. Elam, *ACS Nano* **5**, 4600 (2011).
17. S.H. Kim, M.J. Misner, L. Yang, O. Gang, B.M. Ocko, T.P. Russell, *Macromolecules* **39**, 8473 (2006).
18. Y. Zhao, K. Thorkelsson, A.J. Mastroianni, T. Schilling, J.M. Luther, B.J. Rancatore, K. Matsunaga, H. Jinnai, Y. Wu, D. Poulsen, J.M.J. Fréchet, A.P. Alivisatos, T. Xu, *Nat. Mater.* **8**, 979 (2009).
19. H. Yi, X.-Y. Bao, R. Tiberio, H.-S.P. Wong, *Nano Lett.* **15**, 805 (2015).
20. C.T. Black, R. Ruiz, G. Breyta, J.Y. Cheng, M.E. Colburn, K.W. Guarini, H.-C. Kim, Y. Zhang, *IBM J. Res. Dev.* **51**, 605 (2007).
21. S. Xiao, X. Yang, E.W. Edwards, Y.-H. La, P.F. Nealey, *Nanotechnology* **16**, S324 (2005).
22. X. Yang, L. Wan, S. Xiao, Y. Xu, D.K. Weller, *ACS Nano* **3**, 1844 (2009).
23. J.Y. Cheng, C.A. Ross, "Block Copolymer Lithography for Magnetic Device Fabrication," in *Polymer Thin Films*, Series in Soft Condensed Matter, vol. 1, O.K.C. Tsui, T.P. Russell, Eds. (World Scientific, Singapore, 2008), chap. 4, p. 77.
24. M. Guenther, D. Kuckling, C. Corten, G. Gerlach, J. Sorber, G. Suchaneck, K. Arndt, *Sens. Actuators B* **126**, 97 (2007).
25. C.K. Jeong, H.M. Jin, J.-H. Ahn, T.J. Park, H.G. Yoo, M. Koo, Y.-K. Choi, S.O. Kim, K.J. Lee, *Small* **10**, 213 (2014).
26. Y. Kang, J.J. Walish, T. Gorishnyy, E.L. Thomas, *Nat. Mater.* **6**, 957 (2007).
27. Q. Zhang, A. Cirpan, T.P. Russell, T. Emrick, *Macromolecules* **42**, 1079 (2009).
28. S.J. Metz, J. Potreck, M.H.V. Mulder, M. Wessling, *Desalination* **148**, 303 (2002).
29. C. Fonseca, M. Somervell, S. Scheer, Y. Kuwahara, K. Nafus, R. Gronheid, S. Tarutani, Y. Enomoto, *Proc. SPIE 7640, Opt. Microlithogr. XXIII*, M.V. Dusa, W. Conley, Eds. (SPIE, Bellingham, WA, 2010) p. 76400E.
30. C. Sinturel, F.S. Bates, M.A. Hillmyer, *ACS Macro Lett.* **4**(9), 1044 (2015).
31. H.-C. Kim, S.-M. Park, W.D. Hinsberg, *Chem. Rev.* **110**, 146 (2010).
32. P.A.R.J. Delgadillo, R. Gronheid, C.J. Thode, H. Wu, Y. Cao, M. Neisser, M. Somervell, K. Nafus, P.F. Nealey, *J. Micro/Nanolithogr. MEMS MOEMS* **11**, 031302 (2012).
33. W. Bai, A.F. Hannon, K.W. Gotrik, H.K. Choi, K. Aissou, G. Liontos, K. Ntetsikas, A. Alexander-Katz, A. Avgeropoulos, C.A. Ross, *Macromolecules* **47**, 6000 (2014).

https://doi.org/10.1557/mrs.2016.1 Published online by Cambridge University Press

34. K. Aissou, H.K. Choi, A. Nunns, I. Manners, C.A. Ross, *Nano Lett.* **13**, 835 (2013).
35. W.I. Park, Y. Kim, J.W. Jeong, K. Kim, J.-K. Yoo, Y.H. Hur, J.M. Kim, E.L. Thomas, A. Alexander-Katz, Y.S. Jung, *Sci. Rep.* **3**, 3190 (2013).
36. J.Y. Cheng, A.M. Mayes, C.A. Ross, *Nat. Mater.* **3**, 823 (2004).
37. I. Bita, J.K.W. Yang, Y.S. Jung, C.A. Ross, E.L. Thomas, K.K. Berggren, *Science* **21**, 939 (2008).
38. S.O. Kim, H.H. Solak, M.P. Stoykovich, N.J. Ferrier, J.J. de Pablo, P.F. Nealey, *Nature* **424**, 411 (2003).
39. R.A. Segalman, H. Yokoyama, E.J. Kramer, *Adv. Mater.* **13**, 1152 (2001).
40. P. Mansky, Y. Liu, E. Huang, T.P. Russell, C. Hawker, *Science* **275**, 1458 (1997).
41. Y. Wu, G. Cheng, K. Katsov, S.W. Sides, J. Wang, J. Tang, G.H. Fredrickson, M. Moskovits, G.D. Stucky, *Nat. Mater.* **3**, 816 (2004).
42. H. Hu, M. Gopinadhan, C.O. Osuji, *Soft Matter* **10**, 3867 (2014).
43. M. Luo, T.H. Epps, *Macromolecules* **46**, 7567 (2013).
44. K.G.A. Tavakkoli, K.W. Gotrik, A.F. Hannon, A. Alexander-Katz, C.A. Ross, K.K. Berggren, *Science* **336**, 1294 (2012).
45. J.K. Bosworth, M.Y. Paik, R. Ruiz, E.L. Schwartz, J.Q. Huang, A.W. Ko, D.-M. Smilgies, C.T. Black, C.K. Ober, *ACS Nano* **2**, 1396 (2008).
46. H. Tsai, J.W. Pitera, H. Miyazoe, S. Bangsaruntip, S.U. Engelmann, C.-C. Liu, J.Y. Cheng, J.J. Bucchignano, D.P. Klaus, E.A. Joseph, D.P. Sanders, M.E. Colburn, M.A. Guillorn, *ACS Nano* **8**, 5227 (2014).
47. D. Sundrani, S.B. Darling, S.J. Sibener, *Nano Lett.* **4**, 273 (2004).
48. R.A. Segalman, A. Hexemer, E.J. Kramer, *Macromolecules* **36**, 6831 (2003).
49. R. Ruiz, H. Kang, F.A. Detcheverry, E. Dobisz, D.S. Kercher, T.R. Albrecht, J.J. de Pablo, P.F. Nealey, *Science* **321**, 936 (2008).
50. M.P. Stoykovich, M. Müller, S.O. Kim, H.H. Solak, E.W. Edwards, J.J. de Pablo, P.F. Nealey, *Science* **308**, 1442 (2005).
51. J.Y. Cheng, C.T. Rettner, D.P. Sanders, H.-C. Kim, W.D. Hinsberg, *Adv. Mater.* **20**, 3155 (2008).
52. A.F. Hannon, Y. Ding, W. Bai, C.A. Ross, A. Alexander-Katz, *Nano Lett.* **14**, 318 (2014).
53. J.-B. Chang, H.K. Choi, A.F. Hannon, A. Alexander-Katz, C.A. Ross, K.K. Berggren, *Nat. Commun.* **5**, 3305 (2014).
54. G.S. Khaira, J. Qin, G.P. Garner, S. Xiong, L. Wan, R. Ruiz, H.M. Jaeger, P.F. Nealey, J.J. de Pablo, *ACS Macro Lett.* **3**, 747 (2014).
55. J.K.W. Yang, Y.S. Jung, J.-B. Chang, R.A. Mickiewicz, A. Alexander-Katz, C.A. Ross, K.K. Berggren, *Nat. Nanotechnol.* **5**, 256 (2010).
56. Y.S. Jung, C.A. Ross, *Nano Lett.* **7**, 2046 (2007).
57. C.-C. Liu, P.F. Nealey, A.K. Raub, P.J. Hakeem, S.R.J. Brueck, E. Han, P. Gopalan, *J. Vac. Sci. Technol. B* **28**, C6B30 (2010).
58. J.Y. Cheng, D.P. Sanders, H.D. Truong, S. Harrer, A. Friz, S. Holmes, M. Colburn, W.D. Hinsberg, *ACS Nano* **4**, 4815 (2010).
59. C.M. Bates, T. Seshimo, M.J. Maher, W.J. Durand, J.D. Cushen, L.M. Dean, G. Blachut, C.J. Ellison, C.G. Willson, *Science* **338**, 775 (2012).
60. E. Kim, W. Kim, K.H. Lee, C.A. Ross, J.G. Son, *Adv. Funct. Mater.* **24**, 44, 6981 (2014).
61. S.W. Hong, W. Gu, J. Huh, B.R. Sveinbjornsson, G. Jeong, R.H. Grubbs, T.P. Russell, *ACS Nano* **7**, 9684 (2013).
62. V. Olszowka, M. Hund, V. Kuntermann, S. Scherdel, L. Tsarkova, A. Böker, *ACS Nano* **3**, 1091 (2009).
63. C. Osuji, P.J. Ferreira, G. Mao, C.K. Ober, J.B. Vander Sande, E.L. Thomas, *Macromolecules* **37**, 9903 (2004).
64. G. Singh, K.G. Yager, B. Berry, H.-C. Kim, A. Karim, *ACS Nano* **6**, 10335 (2012).
65. T. Hashimoto, J. Bodycomb, Y. Funaki, K. Kimishima, *Macromolecules* **32**, 952 (1999).
66. G. Cui, M. Fujikawa, S. Nagano, K. Shimokita, T. Miyazaki, S. Sakurai, K. Yamamoto, *Macromolecules* **47**, 5989 (2014).
67. D.E. Angelescu, J.H. Waller, D.H. Adamson, P. Deshpande, S.Y. Chou, R.A. Register, P.M. Chaikin, *Adv. Mater.* **16**, 1736 (2004).
68. C. Tang, W. Wu, D.-M. Smilgies, K. Matyjaszewski, T. Kowalewski, *J. Am. Chem. Soc.* **133**, 11802 (2011).
69. M.S. Onses, A. Ramírez-Hernández, S.-M. Hur, E. Sutanto, L. Williamson, A.G. Alleyne, P.F. Nealey, J.J. de Pablo, J.A. Rogers, *ACS Nano* **8**, 6606 (2014).
70. H. Hu, Y. Choo, X. Feng, C.O. Osuji, *Macromol. Rapid Commun.* **36**, 1290 (2015).
71. A. Böker, H. Elbs, H. Hänsel, A. Knoll, S. Ludwigs, H. Zettl, V. Urban, V. Abetz, A.H.E. Müller, G. Krausch, *Phys. Rev. Lett.* **89**, 135502 (2002).
72. I.W. Hamley, *Nanotechnology* **14**, R39 (2003).
73. K.-H. Tu, W. Bai, G. Liontos, K. Ntetsikas, A. Avgeropoulos, C.A. Ross, *Nanotechnology* **26**, 375301 (2015).
74. J.Y. Cheng, C.A. Ross, V.Z.-H. Chan, E.L. Thomas, R.G.H. Lammertink, G.J. Vancso, *Adv. Mater.* **13**, 1174 (2001).
75. T. Thurn-Albrecht, J. Schotter, G.A. Kastle, N. Emley, T. Shibauchi, K. Guarini, C.T. Black, M.T. Tuominen, T.P. Russell, *Science* **290**, 2126 (2000).
76. C.T. Black, K.W. Guarini, R.L. Sandstrom, S. Yeung, Y. Zhang, "Formation of Nanometer-Scale Dot Arrays from Diblock Copolymer Templates," *Mater. Res. Soc. Symp. Proc.* **728**, S.C. Moss, Ed. (Materials Research Society, Warrendale, PA, 2002), p. S4.9.
77. D.O. Shin, J.H. Mun, G.-T. Hwang, J.M. Yoon, J.Y. Kim, J.M. Yun, Y.-B. Yang, Y. Oh, J.Y. Lee, J. Shin, K.J. Lee, S. Park, J.U. Kim, S.O. Kim, *ACS Nano* **7**, 8899 (2013).
78. J.Y. Kim, B.H. Kim, J.O. Hwang, S.-J. Jeong, D.O. Shin, J.H. Mun, Y.J. Choi, H.M. Jin, S.O. Kim, *Adv. Mater.* **25**, 1331 (2013).
79. F. Rose, J.K. Bosworth, E.A. Dobisz, R. Ruiz, *Nanotechnology* **22**, 035603 (2011).
80. K. Thorkelsson, A.J. Mastroianni, P. Ercius, T. Xu, *Nano Lett.* **12**, 498 (2012).
81. J.W. Jeong, Y.H. Hur, H.-J. Kim, J.M. Kim, W.I. Park, M.J. Kim, B.J. Kim, Y.S. Jung, *ACS Nano* **7**, 6747 (2013).
82. P.W. Majewski, A. Rahman, C.T. Black, K.G. Yager, *Nat. Commun.* **6**, 7448 (2015).
83. J.G. Son, A.F. Hannon, K.W. Gotrik, A. Alexander-Katz, C.A. Ross, *Adv. Mater.* **23**, 634 (2011).
84. S.W. Hong, J. Huh, X. Gu, D.H. Lee, W.H. Jo, S. Park, T. Xu, T.P. Russell, *Proc. Natl. Acad. Sci. U.S.A.* **109**, 1402 (2012).
85. S. Vignolini, N.A. Yufa, P.S. Cunha, S. Guldin, I. Rushkin, M. Stefik, K. Hur, U. Wiesner, J.J. Baumberg, U. Steiner, *Adv. Mater.* **24**, OP23 (2012).
86. Q. Peng, Y.-C. Tseng, S.B. Darling, J.W. Elam, *Adv. Mater.* **22**, 5129 (2010).
87. C. Mendoza, T. Pietsch, J.S. Gutmann, D. Jehnichen, N. Gindy, A. Fahmi, *Macromolecules* **42**, 1203 (2009).
88. S.C. Warren, L.C. Messina, L.S. Slaughter, M. Kamperman, Q. Zhou, S.M. Gruner, F.J. DiSalvo, U. Wiesner, *Science* **320**, 1748 (2008).
89. J. Kao, K. Thorkelsson, P. Bai, Z. Zhang, C. Sun, T. Xu, *Nat. Commun.* **5**, 4053 (2014).
90. Y.-C. Tseng, S.B. Darling, *Polymers (Basel)* **2**, 470 (2010).
91. Y.S. Jung, W. Jung, C.A. Ross, *Nano Lett.* **8**, 2975 (2008).
92. C.T. Black, *Appl. Phys. Lett.* **87**, 163116 (2005).
93. J.G. Son, M. Son, K.-J. Moon, B.H. Lee, J.-M. Myoung, M.S. Strano, M.-H. Ham, C.A. Ross, *Adv. Mater.* **25**, 4723 (2013).
94. C.T. Black, K.W. Guarini, Y. Zhang, H. Kim, J. Benedict, E. Sikorski, I.V. Babich, K.R. Milkove, *IEEE Electron Device Lett.* **25**, 622 (2004).
95. W.I. Park, B.K. You, B.H. Mun, H.K. Seo, J.Y. Lee, S. Hosaka, Y. Yin, C.A. Ross, K.J. Lee, Y.S. Jung, *ACS Nano* **7**, 2651 (2013).
96. B.K. You, W.I. Park, J.M. Kim, K.-I. Park, H.K. Seo, J.Y. Lee, Y.S. Jung, K.J. Lee, *ACS Nano* **8**, 9492 (2014).
97. C.K. Jeong, K.M. Baek, S. Niu, T.W. Nam, Y.H. Hur, D.Y. Park, G.-T. Hwang, M. Byun, Z.L. Wang, Y.S. Jung, K.J. Lee, *Nano Lett.* **14**, 7031 (2014).
98. H.S. Lim, J.-H. Lee, J.J. Walish, E.L. Thomas, *ACS Nano* **6**, 8933 (2012).
99. D. Zhao, J. Feng, Q. Huo, N. Melosh, G.H. Fredrickson, B.F. Chmelka, G.D. Stucky, *Science* **279**, 5350 (1998).
100. J.L. Hedrick, R.D. Miller, C.J. Hawker, K.R. Carter, W. Volksen, D.Y. Yoon, M. Trollsås, *Adv. Mater.* **10**, 1049 (1998).
101. W.A. Phillip, R.M. Dorin, J. Werner, E.M.V. Hoek, U. Wiesner, M. Elimelech, *Nano Lett.* **11**, 2892 (2011).
102. S.Y. Yang, J. Park, J. Yoon, M. Ree, S.K. Jang, J.K. Kim, *Adv. Funct. Mater.* **18**, 1371 (2008).
103. E.A. Jackson, M.A. Hillmyer, *ACS Nano* **4**, 3548 (2010).
104. C. Guo, Y.-H. Lin, M.D. Witman, K.A. Smith, C. Wang, A. Hexemer, J.W. Strzalka, E.D. Gomez, R. Verduzco, *Nano Lett.* **13** (6), 2957 (2013).
105. A.E. Javier, S.N. Patel, D.T. Hallinan, V. Srinivasan, N.P. Balsara, *Angew. Chem. Int. Ed. Engl.* **50**, 9848 (2011).
106. M.C. Orilall, U. Wiesner, *Chem. Soc. Rev.* **40**, 520 (2011).
107. A. Checco, A. Rahman, C.T. Black, *Adv. Mater.* **26**, 886 (2014).
108. A. Rahman, A. Ashraf, H. Xin, X. Tong, P. Sutter, M.D. Eisaman, C.T. Black, *Nat. Commun.* **6**, 5963 (2015).
109. M.L. Adams, A. Lavasanifar, G.S. Kwon, *J. Pharm. Sci.* **92**, 1343 (2003).
110. A.C. Balazs, T. Emrick, T.P. Russell, *Science* **314**, 1107 (2006).
111. M.R. Bockstaller, R.A. Mickiewicz, E.L. Thomas, *Adv. Mater.* **17**, 1331 (2005).
112. J.J. Chiu, B.J. Kim, E.J. Kramer, D.J. Pine, *J. Am. Chem. Soc.* **127**, 5036 (2005).
113. S. Guldin, M. Kolle, M. Stefik, R. Langford, D. Eder, U. Wiesner, U. Steiner, *Adv. Mater.* **23**, 3664 (2011).
114. H.-Y. Hsueh, H.-Y. Chen, Y.-C. Hung, Y.-C. Ling, S. Gwo, R.-M. Ho, *Adv. Mater.* **25**, 1780 (2013).
115. Y. Tao, B. McCulloch, S. Kim, R.A. Segalman, *Soft Matter* **5**, 4219 (2009).
116. S.B. Darling, *Energy Environ. Sci.* **2**, 1266 (2009). □

https://doi.org/10.1557/mrs.2016.1 Published online by Cambridge University Press